Imaging Burned Areas and Fire Severity in Mediterranean Fragmented Ecosystems Using Sentinel-1 and Sentinel-2: The Case Study of Tortoli–Ogliastra Fire (Sardinia)

Rosa Lasaponara, Carmen Fattore, and Giuseppe Modica

***Abstract*— The study aims to explore the added value of the joint use of Sentinel-1 (S1) and Sentinel-2 (S2) data for assessing burn severity in heterogeneous, fragmented ecosystems. The importance of this aim lies in the fact that for both S2 and S1 (as for all the synthetic aperture radar (SAR) C-bands), the impact of fire was found to cause ambiguous effects in complex and fragmented ecosystems. For our investigation, the effectiveness of S1 and S2 fire metrics was first statistically analyzed using ISODATA coupled with field surveys conducted for a fire that occurred on 13 July 2019 in Sardinia. Later, to automatically map burn areas and categorize fire severity, S1 and S2 fire metrics were integrated through a multilevel classification performed at a pixel and feature level. Results were successful (accuracy higher than 94%) compared with independent data sets and in situ investigations.**

***Index Terms*— Burned area, fire severity, Mediterranean shrubs, multilevel classification, spatial autocorrelation, synthetic aperture radar (SAR), wildfires.**

I. Introduction

WILDFIRES are one of the most important causes of environmental degradation, with an increasing impact on a global scale driven and exacerbated by climate change, which induces prolonged drought and increasing temperatures [1], [2], [3], [4].

To contrast wildfire and limit fire incidence, current and future challenges deal with enhancing social and ecological resilience and improving timely and reliable information on the fire occurrence and caused damage.

Earth observation (EO) technologies, particularly the Copernicus program and Sentinel missions [5], [6], [7] can effectively support new fire monitoring applications from a local up to global scale, from pre-fire risk assessment to fire detection, from the mapping of burned areas (as binary identification to discriminate fire affected from fire unaffected pixels) to the estimation of burn/fire severity (categorization of the degree of consumption of vegetation and surface soil organic matter [8]) considered one of the most critical information needed immediately after the fire to set damage-mitigation strategies. Fire severity metrics are directly proportional to the degree of burn and, in turn, to the level of damage. In contrast, the mapping of burned areas is generally referred to as their fire perimeter. Severity metrics (including satellite-derived ones) are typically based on empirical fixed thresholds directly linked to the fire effects observed in the field within the fire perimeter.

Over the years, satellite optical data were widely used to map burned areas and fire severity, providing good accuracy (except in heterogeneous ecosystems) [see, for example [9], [10] and reference therein quoted]. In contrast, synthetic aperture radar (SAR) sensors have been less used due to the less availability of free data (before the launch of S1) and the major complexity of data processing, even if SAR systems provide helpful data for discriminating changes and disturbances in vegetation. Even if, recently, SAR-based fire analyses are increasing [11], [12], [13], [14], [15], [16], [17], [18], [19], [20], [21], [22], [23], [24], [25], [26], [27]. SAR systems offer incoherent (amplitude) and coherent data to perform change detection (CD) compared to optical data. In coherent CD (CCD), the radar images are compared in amplitude and phase, whereas InCoherent CD (ICCD) is based only on amplitude analyses. ICCD was recently carried out by Mastro et al. [12] for obtaining burned area mapping as a binary discrimination of burned from unburnt areas. Obviously, this binary approach [12] is unsuitable for fire severity estimation that requires mandatory categorization of the degrees of fire effect generally approached using incoherent CD. This is mainly due to the fact that scattering variations occur after a fire event due to the loss in vegetation cover, and these variations are directly proportional to the degree of burn. ICCDs for fire investigations are mainly based on metrics based on fixed thresholds linked to the fire effects observed in the field, as successfully made [14] for the SAR L-band to quantify fire damage levels in different continents, environments, ecosystems, and vegetation types. Whereas, up to now, for the SAR C-band, the impact of fire on the backscattering coefficient was actually found to cause ambiguous effects [10] (as shown in Table I) in different ecosystems because it is influenced by forest structure, which is the main factor influencing the backscatter.

Therefore, Tanase et al. [14] suggested using additional information on forest structures to improve the SAR-based burn estimation. Moreover, SAR backscattering tends to exhibit temporal decorrelation, making identifying fire features complex. On the other hand, in fragmented ecosystems, the

Manuscript received 18 July 2023; revised 25 September 2023; accepted 30 September 2023. Date of publication 17 October 2023; date of current version 31 October 2023. *(Corresponding author: Giuseppe Modica.)*

Rosa Lasaponara and Carmen Fattore are with the Institute of Methodologies for Environmental Analysis, National Research Council, Tito, 85050 Potenza, Italy (e-mail: lasaponara@imaa.cnr.it).

Giuseppe Modica is with the Department of Veterinary Sciences, University of Messina, 98168 Messina, Italy (e-mail: giuseppe.modica@unime.it).

Digital Object Identifier 10.1109/LGRS.2023.3324945

TABLE I
ECOSYSTEMS/GEOGRAPHICAL AREAS WHERE AMBIGUOUS EFFECTS HAVE BEEN OBSERVED IN THE C-BAND BACKSCATTERING COEFFICIENT FOR FIRE-AFFECTED AREAS ADAPTED FROM TANASE et al. [14]

Ecosystems/geographical areas	C-band VH	C-band VV
Tropical forest		Strong decrease
Temperate Region	Decrease	
Boreal forest		High increase
Australian woodland and open forest	Decrease	Increase
African	Decrease	Decrease

fixed thresholds commonly used for S2 metrics to categorize fire severity seem unsuitable.

To contribute to this issue, the effectiveness of several S1 and S2 fire severity metrics was assessed in a fragmented ecosystem of Sardinia (Italy). Finally, S1 and S2 fire metrics were integrated through a multilevel classification to map burned areas and fire severity automatically.

II. STUDY AREA AND DATA SETS

The fire event that occurred in Sardinia on 13 July 2019 near Tortoli, in Ogliastra, was selected as a test case. The fire affected around 800 hectares of Mediterranean shrubs (mainly brush, bush, and pasture) classified in the Copernicus EFFIS system [1] as chaparral fuel, i.e., vegetation primarily consisting of tangled shrubs and thorny bushes. For the purpose of our investigation, for both S1 and S2, the most common indices were adopted; in particular, for S2, the normalized burn ratio (NBR) index [12] was computed using the following equation:

$$\mathrm{NBR} = (\mathrm{B8} - \mathrm{B12})/(\mathrm{B8} + \mathrm{B12}). \tag{1}$$

NBR is particularly sensitive to the changes in the amount of live green vegetation, moisture content, and some soil conditions that may occur after a fire, such as ash, the reduced transpiration of vegetation, and the increased surface temperature due to the loss of vegetation cover. All these effects increase the reflectance in mid-infrared [22] and reduce surface reflectance in near-infrared and are better reflected considering the pre/post-burn NBR index difference (dNBR) in the following equation:

$$\mathrm{dNBR} = \mathrm{NBR}_{\text{pre-fire}} - \mathrm{NBR}_{\text{post-fire}}. \tag{2}$$

For S1, we adopted the radar burn ratio (RBR) computed as in (3), the radar burn difference (RBD) as in (4), and the Radar Forest Degradation Index (RFDI) computed as in (5)

$$\mathrm{RBR}_{xy} = \text{Post-fire\_av\_backscatter}_{xy} \big/ \text{Pre-fire\_av\_backscatter}_{xy} \tag{3}$$

$$\mathrm{RBD}_{xy} = \text{Post-fire\_av\_backscatter}_{xy} - \text{Pre-fire\_av\_backscatter}_{xy} \tag{4}$$

$$\mathrm{RFDI} = (\mathrm{VV} - \mathrm{VH})\big/(\mathrm{VH} + \mathrm{VV}). \tag{5}$$

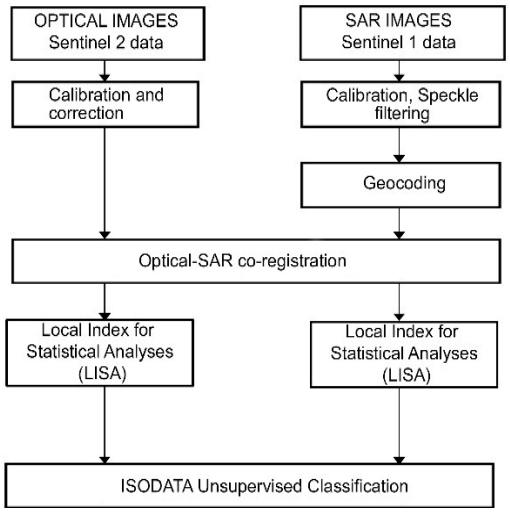

Fig. 1. General flowchart of the proposed data processing.

Both RBR and RBD are calculated for a specific polarization [18], averaging several pre- and post-fire scenes acquired in dry conditions as in [15] to reduce SAR noise and preserve spatial detail. The selection of the number of SAR images to average is based on the meteorological conditions to avoid misclassification due to precipitations and soil moisture.

The RFDI was analyzed [see (6)] as the difference between pre and post-fire maps

$$\mathrm{dRFDI} = \mathrm{RFDI}_{\text{pre-fire}} - \mathrm{RFDI}_{\text{post-fire}}. \tag{6}$$

III. METHOD

A. Analyses of S1 and S2 Fire Severity Metrics

The analyses of the effectiveness of fire severity metrics for both S1 and S2 were carried out using ISODATA unsupervised classification (Fig. 1) in order to overcome the issue linked to the ambiguous effects observed in S2 [9], [10] and S1 [16] fire metric in a heterogeneous, fragmented ecosystem. The use of a cluster-based classification (as ISODATA or other similar approaches) maintains the clear and immediate physical meaning of the investigated fire metrics. It makes the interpretation easier without using fixed thresholds that the local and geographical conditions can obviously limit. ISODATA was also adopted to limit the human intervention in setting up the algorithm parameters as much as possible. The importance of applying unsupervised classification is that: 1) it is an automatic process, which requires only a minimal amount of initial input compared with supervised data processing; 2) classes do not have to be defined a priori; and 3) unknown feature classes may be discovered. Several unsupervised classification algorithms are commonly used in remote sensing, including: 1) K-means clustering and 2) ISODATA, which are pretty similar. In both, the user has only to indicate: 1) the number of predefined classes (clusters) and 2) the number of iterations to be carried out.

Considering that the EFFIS system and Copernicus EMS Rapid Mapping utilize five and three classes of fire severity, respectively, wherein the number of the predefined classes (clusters) was set at 6 and 4 to make comparable the S1 and S2 outputs with the Copernicus products. This enabled us to have

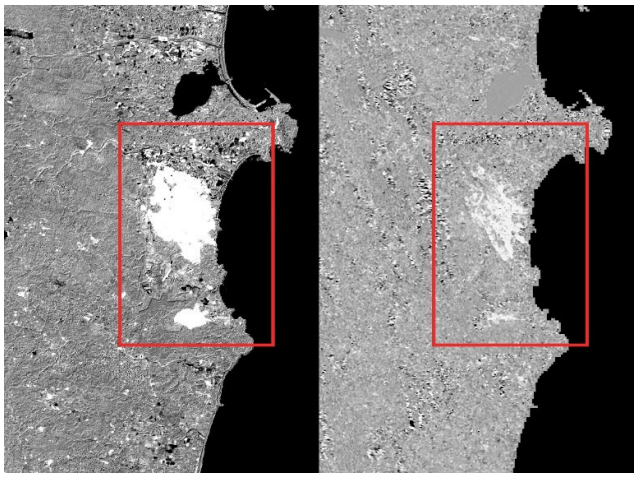

Fig. 2. Images show satellite-based fire severity metrics: (on the left) S2 dNBR and (on the right) S1 RBD. Brighter pixels are related to the fire event that occurred in Sardinia on 13 July 2019 near Tortoli, in Ogliastra.

TABLE II

DETAIL OF DATA USED FOR THIS STUDY: DATES OF THE SATELLITE ACQUIRED BEFORE AND AFTER THE FIRE IN A DESCENDING PASS, BY SENSOR S1-A AND S1-B, IN THE VV, VH POLARIZATION WITH AN INCIDENCE ANGLE RANGING FROM 30.6° TO 46.3° AND RESOLUTION AT 20 × 22 m (IN RANGE × AZIMUTH). THE TYPE OF PRODUCT USED IS GRDH. THE DATA WERE ACQUIRED AROUND 05 A.M. (DESCENDING). S1 AND S2 WERE RESAMPLED AT 10 m THROUGH THE BILINEAR INTERPOLATION METHOD

Pre-Fire	Post-Fire
S1_A_IW 2019/06/17 05:28:47	S1_A_IW 2019/07/23 05:28:49
S1_B_IW 2019/06/23 05:28:08	S1_A_IW 2019/07/29 05:28:10
S1_A_IW 2019/06/29 05:28:48	S1_A_IW 2019/08/04 05:28:50
S1_A_IW 2019/07/11 05:28:48	S1_B_IW 2019/08/10 05:28:11
S2_A_MSI_Level-1C 2019/07/13 10:10:31	S2_A_MSI_Level-1C 2019/07/23 10:10:31

five and three classes for fire severity categorization potentially and one for other targets (unburnt areas, such as water, remains of cloud contamination, etc.). Of course, the six or four classes set in advance are the maximum that can be identified; the number actually found depends on the image statistics.

Fig. 2 shows S2 dNBR and S1 RBD maps where pixels brighter than the context are related to fire-affected areas. Table II lists S1 and S2 data (both resampled at 10 m) used for this study. Fig. 3 shows the ISODATA results from S2 dNBR (on the top) and S1 RBD (on the bottom). The ISODATA outputs from the S1-RBD classification show that this fire metric categorizes a large portion of the image as fire-damaged (mainly yellow and orange classes). Similar behavior has been observed for all the other S1-based fire severity metrics. The ISODATA outputs from the traditional S2-based metric well capture the burned areas (identified in the red and orange classes) with some commission errors that are clearly lower than those obtained from SAR. Therefore, the question is: are C SAR sensors suitable, and to what extent, reliable for

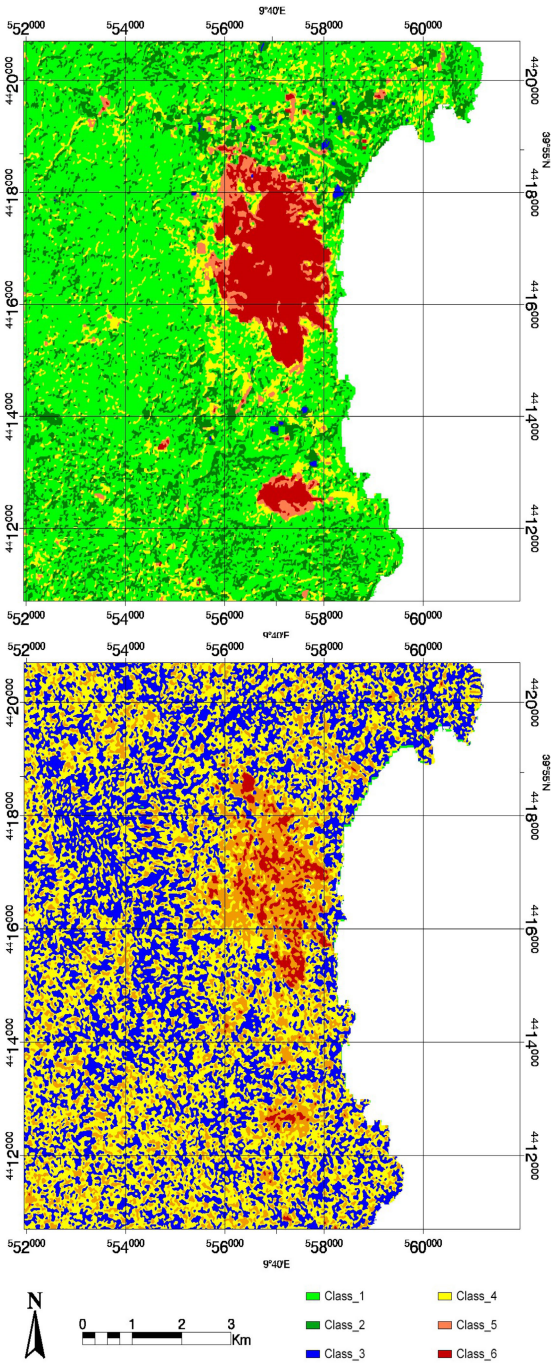

Fig. 3. Images show the ISODATA results from (on the top) S2 dNBR and (on the bottom) S1 RBD.

discriminating fire severity levels? An effort to answer this question is provided in this letter.

B. Fire Severity Categorization

The approach devised to map burned areas and assess fire severity is based on results previously obtained by the same author group using LISA coupled with ISODATA to process S2 [9] in a fragmented ecosystem or S1 [16] in a homogeneous area. In both of these studies, using LISA enabled the enhancement of fire-induced changes, made more evident by enhancing texture variations and/or by the presence of edges and clusters. In this study, ISODATA has been selected to

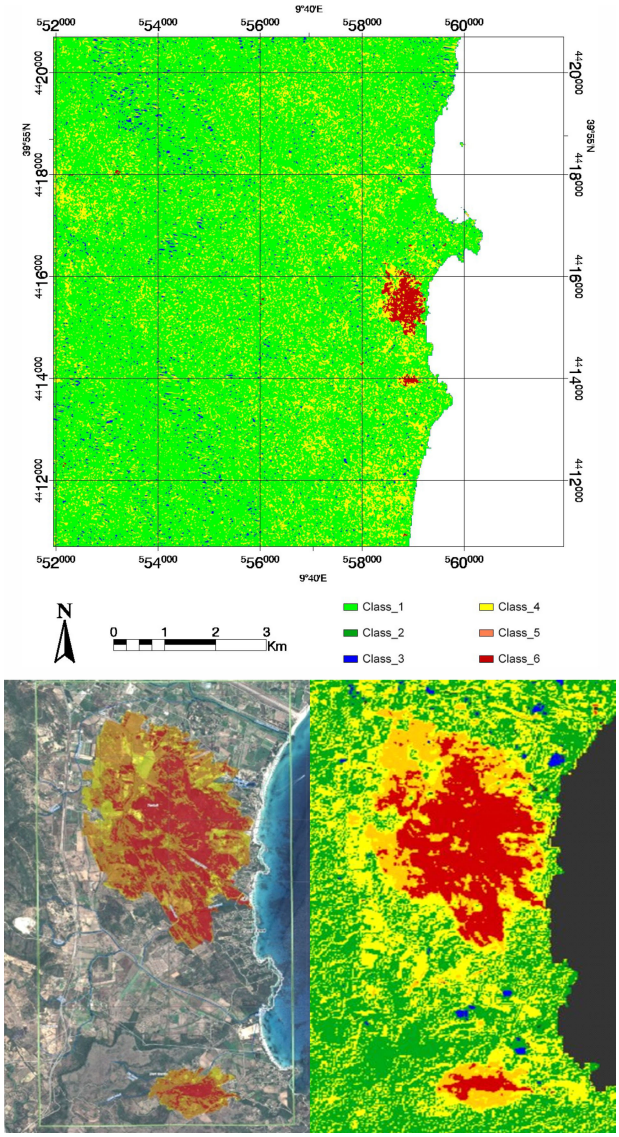

Fig. 4. On the top: joint classification of Moran of S1 RBR and S2 dNBR (herein denoted as feature level classification) 10 m spatial resolution. On the bottom right, ISODATA classification from the joint use of S1 RBR and S2 dNBR at the pixel (10 m spatial resolution) level at 1:100 000 spatial scale. On the bottom left, the Burned area (pixel at 2 m) from the EMS Rapid Mapping [27].

"manipulate" fire metrics, "preserving" their physical meaning linked to the geophysical parameters under investigation.

To exploit the complementarity of S1 and S2 sensors, a data fusion approach was adopted at pixel and feature levels. Both S1 and S2 fire metrics were stacked together to be reclassified at pixel and feature levels.

The classification at the pixel level is obtained from the joint processing of the together stacked S1 and S2 fire severity metrics (all resampled at 10 m of pixel resolution). As a whole, three different classifications were run obtained based on the joint use of: 1) S2 dNBR and S1 RBD [(2) and (3)]; 2) S2 dNBR and S1 RBR [(2) and (4)]; and 3) S2 dNBR and S1 difference of the RFDI obtained from the difference of pre and post-fire maps [(2) and (6)].

Feature-level data are generally adopted for decision analysis, and fusion results are expected to provide new features more suitable for decision analysis. The feature-level classification is obtained from the feature-level data fusion approach, based on the joint use of fire features obtained from the classification of each metric obtained from each sensor. So, as in the case of the pixel-level classification, the final products are three.

TABLE III

RESULTS OBTAINED FROM THE PIXEL-LEVEL CLASSIFICATION OF S1 RBR AND S2 DNBR (BOTTOM RIGHT IN FIG. 4) WERE COMPARED WITH THE DAMAGE ASSESSMENT PROVIDED BY THE COPERNICUS EMS RAPID MAPPING [25] FOR THE TWO CLASSES DENOTED AS DESTROYED AND DAMAGED. IN CONTRAST, THE CLASS DENOTED AS PROBABLY DAMAGED WAS NOT CONSIDERED BECAUSE OF ITS UNCLEAR PHYSICAL MEANING

Burnt area [ha]	Destroyed [ha]	Damaged [ha]	Tot [ha]
EMSR 371 map	262.49	362.30	624.79
RBR+dNBR	253.54	383.49	637.03
Accuracy			94%

IV. RESULTS

Outputs from all the classifications were overlapped on Google Earth and compared with the Very High-Resolution optical satellite Pléiades S1A/B imagery acquired on 18 July 2019, immediately after the fire occurrence and used by Copernicus EMS [28] for mapping burned areas and fire severity. The Copernicus EMS provides support (if institutional authorities request) immediately following a disaster. In the current case, the service was requested and activated on 17 July. It provided the mapping of burned areas and different levels of fire damage as obtained using Pléiades S1A/B (see Fig. 4). EMS estimated that the area affected by the fire was around 665.5 ha and identified the diverse levels of fire damage categorized as destroyed (in red), damaged (in orange), and possibly damaged (in yellow).

Results from our analysis pointed out that as follows.

1) The use of LISA enabled a better identification and delineation of the fire-affected pixels, not only for S2 (thus confirming the already published output [12]) but also for S1-based fire metrics.
2) For the mapping of burned areas (fire perimeter), the best performance was obtained from the classification of Moran applied to RBR in the VH polarization. Fig. 4 shows (on the top) the zoom of the results from the joint classification of Moran of S2 dNBR and S1 RBD VH polarization (herein indicated as feature-level classification).
3) For the fire severity categorization, the best performance was obtained from the classification of Moran applied to RBR in the VH polarization performed at the pixel level. As a whole, the satellite sentinel-based results (at 10 m of spatial resolution) were successfully compared with the independent fire map provided by the Copernicus EMS (from Pléiades S1A/B data at 2 m of spatial resolution) (Table III) [27].

V. DISCUSSION AND CONCLUSION

The study illustrates the potential of the synergic use of S1 and S2 for speditive and effective fire severity mapping, exploiting the complementarity of the two sensors.

The satellite sentinel-based results (at 10 m of spatial resolution) were successfully compared with the independent

fire map provided by the Copernicus EMS (from Pléiades S1A/B data at 2 m of spatial resolution) [28]. The comparison clearly showed the excellent match of the burned areas and fire damage mapped from the Copernicus EMS Rapid Mapping map based on Pléiades S1A/B and the classification obtained from S1 and S2. These results are highly satisfactory considering that the whole area is sparsely vegetated and characterized by a dominant presence of Mediterranean shrubs (mainly brush, bush, and pasture) classified as chaparral fuel [1]. As a whole, results from our analyses clearly pointed out that both of the two proposed approaches (i.e., the joint ISODATA classification of S1 RBD of VH polarization and S2 at pixel and feature level) can be used to detect burned areas and estimate fire severity providing a speditive and accurate characterization with the diverse degrees of fire damage.

Future efforts will be addressed to refine the classification further using the enhancement of fire features (herein obtained by LISA) and artificial intelligence (AI) approaches, which require a significantly large data set to obtain successful results.

ACKNOWLEDGMENT

The activities were carried out within the project FIREurisk, funded by EC (https://fireurisk.eu).

REFERENCES

[1] FAO. *International Cooperation in Wildland Fire Management*. Accessed: Sep. 20, 2023. [Online]. Available: http://www.fao.org/3/y5507e/y5507e02.htm

[2] *Global Wildfire Information System (GWIS)*. Accessed: Oct. 10, 2023. [Online]. Available: https://gwis.jrc.ec.europa.eu

[3] J. Ruiz-Ramos, A. Marino, and C. P. Boardman, "Using sentinel 1-SAR for monitoring long term variation in burnt forest areas," in *Proc. IEEE Int. Geosci. Remote Sens. Symp.*, Jul. 2018, pp. 4901–4904, doi: 10.1109/IGARSS.2018.8518960.

[4] M. Turco, M.-C. Llasat, J. von Hardenberg, and A. Provenzale, "Climate change impacts on wildfires in a Mediterranean environment," *Climatic Change*, vol. 125, nos. 3–4, pp. 369–380, Aug. 2014, doi: 10.1007/s10584-014-1183-3.

[5] G. Otón, R. Ramo, J. Lizundia-Loiola, and E. Chuvieco, "Global detection of long-term (1982–2017) burned area with AVHRR-LTDR data," *Remote Sens.*, vol. 11, no. 18, p. 2079, Sep. 2019, doi: 10.3390/rs11182079.

[6] ESA. *Sentinel Missions*. Accessed: Sep. 20, 2023. [Online]. Available: https://sentinel.esa.int/web/sentinel/missions

[7] *Copernicus Global Land Service, Burnt Area (BA)*. Accessed: Oct. 10, 2023. [Online]. Available: https://land.copernicus.eu/global/products/BA

[8] I. Gitas, G. Mitri, S. Veraverbeke, and A. Polychronaki, "Advances in remote sensing of post-fire vegetation recovery monitoring—A review," in *Remote Sensing of Biomass: Principles and Applications*, L. Fatoyinbo, Ed. London, U.K.: IntechOpen, 2012, pp. 143–177, doi: 10.5772/20571.

[9] R. Lasaponara, B. Tucci, and L. Ghermandi, "On the use of satellite Sentinel 2 data for automatic mapping of burnt areas and burn severity," *Sustainability*, vol. 10, no. 11, p. 3889, Oct. 2018.

[10] R. Lasaponara, A. M. Proto, A. Aromando, G. Cardettini, V. Varela, and M. Danese, "On the mapping of burned areas and burn severity using self organizing map and Sentinel-2 data," *IEEE Geosci. Remote Sens. Lett.*, vol. 17, no. 5, pp. 854–858, May 2020.

[11] G. De Luca, G. Modica, C. Fattore, and R. Lasaponara, "Unsupervised burned area mapping in a protected natural site. An approach using SAR Sentinel-1 data and k-mean algorithm," in *Computational Science and Its Applications—ICCSA* (Lecture Notes in Computer Science), vol. 12253, O. Gervasi, Ed. Cham, Switzerland: Springer, 2020, pp. 63–77.

[12] P. Mastro, G. Masiello, C. Serio, and A. Pepe, "Change detection techniques with synthetic aperture radar images: Experiments with random forests and Sentinel-1 observations," *Remote Sens.*, vol. 14, no. 14, p. 3323, Jul. 2022, doi: 10.3390/rs14143323.

[13] E. Chuvieco et al., "Historical background and current developments for mapping burned area from satellite Earth observation," *Remote Sens. Environ.*, vol. 225, pp. 45–64, May 2019, doi: 10.1016/j.rse.2019.02.013.

[14] M. A. Tanase, M. Santoro, J. de la Riva, F. Prez-Cabello, and T. Le Toan, "Sensitivity of X-, C-, and L-band SAR backscatter to burn severity in Mediterranean pine forests," *IEEE Trans. Geosci. Remote Sens.*, vol. 48, no. 10, pp. 3663–3675, Oct. 2010, doi: 10.1109/TGRS.2010.2049653.

[15] P. Imperatore et al., "Effect of the vegetation fire on backscattering: An investigation based on Sentinel-1 observations," *IEEE J. Sel. Topics Appl. Earth Observ. Remote Sens.*, vol. 10, no. 10, pp. 4478–4492, Oct. 2017, doi: 10.1109/JSTARS.2017.2717039.

[16] R. Lasaponara and B. Tucci, "Identification of burned areas and severity using SAR Sentinel-1," *IEEE Geosci. Remote Sens. Lett.*, vol. 16, no. 6, pp. 917–921, Jun. 2019.

[17] M. Gimeno and J. San-Miguel-Ayanz, "Evaluation of RADARSAT-1 data for identification of burnt areas in Southern Europe," *Remote Sens. Environ.*, vol. 92, no. 3, pp. 370–375, Aug. 2004, doi: 10.1016/j.rse.2004.03.018.

[18] G. Vaglio Laurin, R. Avezzano, V. Bacciu, F. Frate, D. Papale, and M. Virelli, "COSMO-SkyMed potential to detect and monitor Mediterranean maquis fires and regrowth: A pilot study in Capo Figari, Sardinia, Italy," *iForest-Biogeosciences Forestry*, vol. 11, no. 3, pp. 389–395, Jun. 2018, doi: 10.3832/ifor2623-011.

[19] N. H. French, L. L. Bourgeau-Chavez, Y. Wang, and E. S. Kasischke, "Initial observations of Radarsat imagery at fire-disturbed sites in interior Alaska," *Remote. Sens. Environ.*, vol. 68, pp. 89–94, Apr. 1999, doi: 10.1016/S0034-4257(98)00094-7.

[20] G. De Luca, J. M. N. Silva, and G. Modica, "Short-term temporal and spatial analysis for post-fire vegetation regrowth characterization and mapping in a Mediterranean ecosystem using optical and SAR image time-series," *Geocarto Int.*, vol. 37, no. 27, pp. 15428–15462, Dec. 2022, doi: 10.1080/10106049.2022.2097482.

[21] G. De Luca, J. M. N. Silva, and G. Modica, "Regional-scale burned area mapping in Mediterranean regions based on the multitemporal composite integration of Sentinel-1 and Sentinel-2 data," *GIScience Remote Sens.*, vol. 59, no. 1, pp. 1678–1705, Dec. 2022, doi: 10.1080/15481603.2022.2128251.

[22] T. Chu, X. Guo, and K. Takeda, "Remote sensing approach to detect post-fire vegetation regrowth in Siberian boreal larch forest," *Ecological Indicators*, vol. 62, pp. 32–46, Mar. 2016, doi: 10.1016/j.ecolind.2015.11.026.

[23] Y. Ban, P. Zhang, A. Nascetti, A. R. Bevington, and M. A. Wulder, "Near real-time wildfire progression monitoring with Sentinel-1 SAR time series and deep learning," *Sci. Rep.*, vol. 10, no. 1, p. 1322, Jan. 2020, doi: 10.1038/s41598-019-56967-x.

[24] D. Stroppiana et al., "Integration of optical and SAR data for burned area mapping in Mediterranean regions," *Remote Sens.*, vol. 7, no. 2, pp. 1320–1345, Jan. 2015.

[25] C. Fan and S. Myint, "A comparison of spatial autocorrelation indices and landscape metrics in measuring urban landscape fragmentation," *Landscape Urban Planning*, vol. 121, pp. 117–128, Jan. 2014, doi: 10.1016/j.landurbplan.2013.10.002.

[26] R. K. Gibson, A. Mitchell, and H.-C. Chang, "Image texture analysis enhances classification of fire extent and severity using Sentinel 1 and 2 satellite imagery," *Remote Sens.*, vol. 15, no. 14, p. 3512, Jul. 2023, doi: 10.3390/rs15143512.

[27] G. De Luca, G. Modica, J. M. N. Silva, S. Pratico, and J. M. C. Pereira, "Assessing tree crown fire damage integrating linear spectral mixture analysis and supervised machine learning on Sentinel-2 imagery," *Int. J. Digit. Earth*, vol. 16, no. 1, pp. 3162–3198, Dec. 2023, doi: 10.1080/17538947.2023.2243900.

[28] (2019). *Fire in Sardinia, Italy*. European Commission, Joint Research Centre. Accessed: May 23, 2020. [Online]. Available: https://emergency.copernicus.eu/mapping/list-of-components/EMSR371 and http://data.europa.eu/89h/cbeb0f95-1ebd-4b4d-be82-9faa4abc1273

Open Access funding provided by 'Università degli Studi di Messina' within the CRUI CARE Agreement